Voltage Dependence of Carbon - Based Supercapacitors for Pseudocapacitance Quantification

V. Ruiz[†], S. Roldán, I. Villar, C. Blanco[*] and R. Santamaría

Instituto Nacional del Carbón, C.S.I.C., Apdo. 73, 33080-Oviedo, Spain

Abstract.-

In order to understand the participation of electrical double layer and pseudocapacitance to the overall behavior of supercapacitors, a new approach to the analysis of the electrochemical data is proposed. Both the variation of the specific capacitance values and the dependence of these values with the operating voltage window (varying from 0-0.2 V to 0-1 V) were evaluated and used to quantify the contribution arising from each mechanism of energy storage to the total capacitance of the system.

The suitability of the methodology here proposed was tested in various carbon materials (multiwalled carbon nanotubes, a carbon aerogel and two activated carbons), different both in nature and physicochemical characteristics. For all of the carbons studied, the capacitance with an exclusive faradic and non - faradic origin was quantified. Whereas some of the carbons studied showed a behavior close to an ideal Electrical Double Layer Capacitor (EDLC) with virtually no pseudocapacitance contribution (case of the carbon nanotubes), others presented up to a 40 % of pseudocapacitance contribution (case of KOH - activated carbon).

Keywords: Activated carbon, supercapacitors, double layer, pseudocapacitance, voltage dependence

[†] Current address: Centro de Investigación en Nanociencia y Nanotecnología,CIN2 (CSIC). Campus UAB 08193 Bellaterra, Spain. Phone: (+34) 935868531, Fax: (+34) 935868020. E-mail: vanesa.ruiz@cin2.es
[*] Corresponding author: E-mail: clara@incar.csic.es Tel. + 34 985 118994; Fax: + 34 985 297662

1.- INTRODUCTION

Energy storage in electrochemical capacitors occurs via two different mechanisms: the formation of the so-called electrical double layer and pseudocapacitance. The first mechanism is purely electrostatic and no faradic reactions are involved between the solid material and the electrolyte. This is typically found in Electrochemical Double Layer Capacitors (EDLCs), which are usually carbon-based. As stated by Burke [1], the capacitance (*dQ/dV*) in this case is constant and independent of voltage. The second mechanism involves faradic currents from reactions and the resultant charge transfer gives rise to a pseudocapacitance, which generally: *i)* cannot be directly measured *ii)* is utilizable as a capacitance and *iii)* is voltage dependent [1,2]. Nonetheless, there are number of metal oxides pseudocapacitative materials which have a constant capacitance with changing voltage.

There are several alternatives to exploit the mechanism of pseudocapacitance in supercapacitors (SCs): surface electrosorption of ions from the electrolyte, redox reactions of metal oxides (*e.g.* RuO_2 [3]), doping/undoping of active conducting polymer materials (*e.g.* polyaniline, polythiofene [4]), etc. Carbon materials also show a faradic component (e.g. redox reactions of the surface functionalities such as quinone-type functional groups [5,6,7]) together with the electrostatic one. Besides, non-desirable faradic currents may be present in the form of electrolyte decomposition or electrode oxidation. In many situations, the two mechanisms of energy storage act simultaneously and, therefore, their distinction is particularly complicated especially when the interfaces are part of a porous matrix system, thus double layer capacitance (C_{dl}) and pseudocapacitance (C_p) are not coupled in a simple parallel way, adding up their values [2,8,9].

The data obtained from the experimental techniques commonly used to characterize SCs (e.g. cyclic voltammetry) are unable to quantitatively separate the contribution of each mechanism. Many authors have qualitatively evaluated the effect of, for example, oxygen or nitrogen -containing electrode materials on the capacitor´s characteristics through various indirect approaches: (1) evaluating the capacitance of one material before and after removing (or incorporating) surface functionalities (e.g. oxygen removal by heat treatment [6], oxidation [10-12], ammoxidation [13], etc.) or (2) comparing capacitance values in acidic, basic and non-aqueous media [7].The soundness of any of these two approaches might be doubtful as: for case (1) treatments (thermal, oxidative, etc.) of the electrode material would alter its nature at various levels: textural (porosity), electrical (electronic conductivity), chemical (wettability), etc. and for case (2) each electrolytic media has different ionic conductivity, ion transport/diffusion, pore size accessibility, distance separating the charges at the electrode/electrolyte interface [14], electrolyte breakdown window, etc. On top of this, the pseudocapacitance studied in cases (1) and (2) is limited to that of a redox nature, as all the other possibilities (e.g. adsorption of ions, variations in the electrolyte dielectric constant, etc.) are obviated. We are presenting an alternative that does not modify the nature of the active material. The method we propose is inspired by the general definition of pseudocapacitance (measurable capacitance, faradic in origin, dependent on the electrode potential [15]) and a quantitative evaluation of each mechanism of energy storage is pursued. Different materials, including carbon nanotubes, an aerogel, a commercial activated carbon and a chemically activated carbon are used for this. The amounts of C_{dl} and C_p estimated with our model are in good agreement with both the textural and chemical characteristics of the electrode materials evaluated, which would imply the capability of this methodology to be extrapolated to other carbon materials.

Nonetheless, the method would find limitations in those particular cases where the formation of the double layer is voltage-dependent (very narrow micropores combined with high current densities).

2 EXPERIMENTAL

2.1.- Active materials: origin and characterization.-

Various carbon materials (CMs) different in origin and characteristics were used in this study. A carbon aerogel supplied by *Marketech International*, multiwalled carbon nanotubes (MWNTs) supplied by *Sigma-Aldrich*, and two activated carbons, one commercially available (Super-DLC, supplied by *Norit-Chemicals*, obtained by steam activation of natural-based raw materials) and another prepared in our laboratories (A7). This sample was obtained by means of chemical activation of a naphthalene mesophase pitch using KOH as activating agent in a proportion to the pitch (3:1) at 700 °C, following the procedure described in [16].

Physical adsorption of N_2 at 77 K was carried out in order to characterize the porous texture of the porous materials. Isotherms were performed in an *ASAP 2020Micromeritics* volumetric system. The apparent specific surface area was determined from the N_2-adsorption isotherm using the BET equation. The total micropore volume (V_{N2}) and the microporous surface area (S_{mic}) was calculated by applying the Dubinin-Radushkevich (DR) equation to the N_2 isotherm [17]. The total pore volume was obtained from N_2 adsorption at P/P^0 = 0.99, and the volume of mesoporos was calculated by subtracting the total micropore volume (V_{N2}) from the total pore volume. The DFT method was applied to the N_2 adsorption isotherms to determine the total surface area.

The activated carbons were characterized by elemental analyses and the oxygen was determined directly using a LECO-TF-900 furnace coupled to a LECO-CHNS-932 microanalyser. The amount and type of oxygenated functionalities were determined by temperature-programmed decomposition (TPD) under an inert atmosphere (He). The decomposition products were identified using an online mass spectrometer.

2.2.- Electrochemical characterization

The electrochemical performance of the materials was studied from galvanostatic cycling in two-electrode cell configuration and cyclic voltammetry in three-electrode cell configuration. Disk-type electrodes were prepared using a mixture of activate material and polyvinylidene fluoride (PVDF). The resultant electrodes were dried in a vacuum oven at 110 ºC overnight before each experiment. The two-electrode cells were assembled with two disks (12 mm in diameter, ~ 40 mg), a glassy fibrous separator and gold current collectors in a Swagelok®- type cell. Galvanostatic cycling was performed at various current densities (1.0-88.4 mA cm^{-2}). Each cell was cycled at increasing operating voltage windows (starting at 0-0.2 V, gradually increasing to 0-1 V, with 200 mV intervals). Several cells were prepared to obtain reliable and repeatable data. Tests were performed in a *Biologic VMP3* multichannel potentiostat using 1M H_2SO_4 as electrolyte. The specific capacitance (C) of the system was obtained applying the following equation: C (F g^{-1}) = 2 I/m (dV/dt) to the constant current discharge curve (avoiding the ohmic drop), where I is the current in amperes, dV/dt is the slope of the discharge curve and m is the weight of the active material in the lightest electrode.

Cyclic voltammetry (CV) was carried out at 0.2 mV s^{-1} in a three-electrode cell configuration, using a platinum mesh as the counter electrode and $Hg|Hg_2SO_4$ as the reference electrode.

3 RESULTS

3.1.- Active materials characteristics.-

Table 1 summarizes the textural properties of the CMs. The materials studied have apparent BET surfaces areas varying from 210 to 2008 m^2 $g^{-1}$with average pore sizes ranging ~1-2 nm. Two of them, A7 and Super-DLC are highly microporous samples, whereas the aerogel and the MWCNTs are fairly mesoporous. A7 has close to 90 % of its porosity below 2 nm in size. Super-DLC has a significant amount of mesoporosity, showing higher L_0 and V_{meso} values.

Apart from the differences in texture, the set of samples here studied has different chemical properties (Table 1), from materials with very low oxygen content, as the MWNTs, to materials rich in functionalities as the sample A7 with up to 4.50 wt. % in oxygen. The TPD results give complementary information [18]. Upon heating carbon materials, CO_2 evolves at low temperature as a consequence of decomposition of carboxylic groups, lactones and/or anhydrides whereas CO evolution occurs at higher temperatures, due to the decomposition of basic or neutral groups such as phenols, ethers and carbonyl groups. For all of the materials evaluated the amount of groups that evolve as CO is higher than the amount of groups that evolve as CO_2, except for the carbon aerogel were a negligible amount of CO-evolving groups was found.

3.2.-Electrochemical characteristics.-

Figure 1.a shows the galvanostatic charge-discharge cycles obtained for Super-DLC in 1M H_2SO_4 at a fixed current load (1 mA cm^{-2}) at increasing voltage windows (from 0-0.2 V to 0-1 V by increasing 200 mV after each cycle). These cycles show the typical triangular shape attributed to EDLCs [19] where the active material shows a capacitative behavior. However, it can be observed in the graph that there is some slight deviation from ideality when the voltage is increased, this being normally associated to the presence of faradaic currents [2,20]. Figure 1.b shows the specific capacitance values obtained from the galvanostatic experiments performed over a range of current loads (1 to 88 mA cm^{-2}) for each operating voltage (0.2, 0.4, 0.6, 0.8 and 1 V). As can be clearly observed, the capacitance values have a strong dependence on the operating potential. At the lowest current density (1 mA cm^{-2}) the cell stores 120 F g^{-1} at 0.2 V, whereas at 1 V the capacitance value increases to 167 F g^{-1}. This increase could be attributed to a pseudocapacitative component. If capacitance values for Super-DLC (C, F g^{-1}) are plotted versus the voltage window used, ΔV, at each current density load (Figure 2) a clear linear trend was observed for all the current densities evaluated. The capacitance values obtained at 0.2 V at the highest current densities were not included as the influence of the ohmic drop makes the calculation of capacitance more imprecise.

In order to further analyze the experimental data, special attention was paid to the capacitance values obtained at the lowest current density (1 mA cm^{-2}), where it is generally accepted that the kinetic limitations are negligible. Figure 3 displays the specific capacitance values obtained for all the carbon materials tested at varying cell voltages (0.2 – 1 V) for a single current density. For the A7, Super-DLC and Aerogel samples a clear increasing trend is found, whereas MWNTs show negligible dependence of capacitance and cell voltage window. The equation that best fits the experimental

capacitance values has the form of (Eq. 1) for both activated carbons and (Eq. 2) for the Aerogel.

$$C\ (F\ g^{-1}) = a\Delta V + b \qquad \text{(Eq. 1)}$$

$$C\ (F\ g^{-1}) = a\Delta V^2 + b\Delta V + c \qquad \text{(Eq. 2)}$$

Based on the definition of each mechanism of energy storage, the part of the equation independent on the voltage (b in Eq. 1 and c in Eq. 2) was assigned to the capacitance coming from the double layer formation only, C_{dl}, while the part of the equation dependent on the cell voltage, can be assigned to the capacitance of pseudo origin, C_p. These assumptions would not apply in the case of high current densities where the formation of the double layer might be restricted in narrow pores and, therefore, becoming voltage dependence (21,22). Table 2 summarizes the equations that best fit the experimental capacitance values for each carbon material, the corresponding correlation coefficient and the values of C_{dl}, C_p and the contribution of C_p to the total capacitance at each voltage studied. Results corresponding to Super-DLC were fitted to a straight line of the form: $C\ (F\ g^{-1}) = 60\Delta V + 108$, so $C_{dl} = 108\ F\ g^{-1}$and $C_p = 60\Delta V$. Therefore, for the various cell voltages used, it is possible to obtain the C_p values, which are 12 F g^{-1} at 0.2 V, 24 at 0.4 V, 36 at 0.6 V, 48 at 0.8 V and 60 at 1 V. Thus, at 0.2 V, the C_p contribution is as low as 10 %, and increases to 36 % when the cell voltage used is 1 V. The same discussion can be made for the rest of the samples.

MWNTs represent the performance of an ideal EDLC, with a constant capacitance value over the whole range of ΔVs ($C = 17\ F\ g^{-1}$). This can be attributed to its negligible oxygen content (see Table 1) and their well-known electrochemical stability upon cycling; therefore no faradaic contribution is expected.

A7, Super-DLC and Aerogel materials showed double layer capacitance values equal to: 150, 107, and 68 F g^{-1}, respectively. These C_{dl} values increase when increasing surface area of the electrode material and this increase is fairly linear when S_{mic} is taken into account, in agreement with other highly microporous materials (e.g. negligible external surface area) described in the literature [23,24]. The pseudocapacitance contribution (Table 2) was higher for A7 at any voltage window than for the other samples, as a reflection of its higher oxygen content, Table 1. In particular, it has a significantly higher content in CO-evolving groups which are traditionally assigned to a quinone/hydroquinone-like redox activity [25-27].

The calculated C_p value for the carbon Aerogel is very low at low voltage windows, representing only 1 % of the total capacitance at 0.2 V and 5 % at 0.4 V, and it increases up 28 % at 1 V (Table 2). Based on initial oxygen content of the sample, the majority of the oxygen of the sample is in the form of CO_2-evolving groups, which do not contribute to capacitance [6]. The increase of C_p when increasing the voltage window can be attributed to the creation of functionalities upon cycling. It has been demonstrated by our group, as well as others, that electro-oxidation of electrode materials can occur upon cycling [28-30]. The newly introduced functionalities lead to a pseudocapacitance contribution as it has been evidenced in the literature and by some authors.

In order to demonstrate our argument, cyclic voltammograms (CVs) were obtained in a three-electrode configuration (Figure 4). The carbon aerogel (Fig. 4.a) shows a typical rectangular behavior for a range of potential from -0.2 to + 0.2 V vs $Hg|Hg_2SO_4$ (ΔV = 0.4 V), so little pseudocapacitance contribution is expected corroborating the low calculated C_p value. When the voltage window is widened towards -0.4 and +0.4 V vs $Hg|Hg_2SO_4$ (ΔV = 0.8 V), a small bump starts to stand out

(at a potential typical of electrochemically active quinoid groups), particularly during the reduction scan, which is in agreement with the increase in pseudocapacitance observed (see Table 2). For comparison, cyclic voltammogram obtained for sample A7 displays visible redox peaks even at only $\Delta V = 0.4$ V (Figure 4.b); which turn into well-defined peaks centered at approximately -0.2 V (reduction) and -0.03 V (oxidation) when $\Delta V = 0.8$ V. This is in agreement with the significant amount of C_p across the whole range of voltage windows used.

Based on all the information evaluated, it was possible to discern the pseudocapacitance contribution of four types of materials, all different in origin and physicochemical properties; thus this methodology could be allegedly widespread to other type of carbon electrode materials.

4.- Conclusions.-

It was possible to quantify the contribution of each mechanism of energy storage (double layer, C_{dl}, and pseudocapacitative, C_p) to the overall capacitance of various carbon-based supercapacitors based on the relationship between capacitance values (C) and operating voltage window (ΔV).

The quantification of pseudocapacitance was achieved using conventional electrochemical tests and without modification of the samples with chemical or thermal treatments.

C_{dl} was found to follow a linear increase with the microporous surface area of the carbon materials evaluated whereas C_p shows strong correlation to oxygen content. A high pseudocapacitance contribution (as high as 43 %) was found for A7, activated carbon rich in oxygen functionalities, whereas a sample with almost no oxygenated

functionalities and resistant to electro-oxidation as the MWNTs showed a negligible contribution of pseudocapacitance.

Acknowledgements.- Authors acknowledge financial support from the MICINN (Project MAT2010-20601-C02-01). Silvia Roldán thanks MICINN for a FPI predoctoral research grant.

References.

[1] A. Burke, Journal of Power Sources, 91 (2000) 37-50.

[2] B. Conway, Electrochemical Supercapacitors. Scientific Fundamentals and Technological Applications, New york, 1999. p.105

[3] V.D. Patake, C.D. Lokhande, Applied Surface Science, 254 (2008) 2820-2824.

[4] M. Selvakumar, D.K. Bhat, Journal of Applied Polymer Science, 107 (2008) 2165-2170.

[5] T.D. Tran, D. Lenz, K. Kinoshita, M. Droege, Electrochemical properties of carbon aerogel composites, in: D.S.D.D.H.S.B.T.T.Z.Z.M.J. Ginley (Ed.) Materials for Electrochemical Energy Storage and Conversion Ii-Batteries, Capacitors and Fuel Cells, vol. 496, 1998, pp. 607-611.

[6] V. Ruiz, C. Blanco, E. Raymundo-Pinero, V. Khomenko, F. Beguin, R. Santamaria, Electrochimica Acta, 52 (2007) 4969-4973.

[7] H.A. Andreas, B.E. Conway, Electrochimica Acta 51 (2006) 6510-6520.

[8] B.E. Conway, V. Birss, J. Wojtowicz, Journal of Power Sources, 66 (1997) 1-14.

[9] P. Delahay, J. Electroanalytical Chemistry, 21 (1976) 337.

[10] D. Lozano-Castello, D. Cazorla-Amoros, A. Linares-Solano, S. Shiraishi, H. Kurihara, A. Oya, Carbon, 41 (2003) 1765-1775.

[11] C.G. Liu, H.T. Fang, F. Li, M. Liu, H.M. Cheng, Journal of Power Sources, 160 (2006) 758-761.

[12] R. Pietrzak, K. Jurewicz, P. Nowicki, K. Babel, H. Wachowska, Fuel, 86 (2007) 1086-1092.

[13] K. Jurewicz, K. Babel, A. Ziolkowski, H. Wachowska, M. Kozlowski, Fuel Processing Technology, 77 (2002) 191-198.

[14] F. Rafik, H. Gualous, R. Gallay, A. Crausaz, A. Berthon, Journal of Power Sources, 165 (2007) 928-934.
[15] B.E. Conway, W.G. Pell, Journal of Solid State Electrochemistry, 7 (2003) 637-644.
[16] E. Mora, V. Ruiz, R. Santamaria, C. Blanco, A. Granda, R. Menendez, J.M. Juarez-Galan, F. Rodriguez-Reinoso, Journal of Power Sources, 156 (2006) 719-724.
[17] M.M. Dubinin, Cadenhead DA (Ed.), 9 (1975).
[18] F.J.V. G. Tremblay, P.L. Walker, Carbon, 16 (1978) 35.
[19] E. Frackowiak, F. Beguin, ibid.39 (2001) 937-950.
[20] G.-Q. Zhang, Y.-Q. Zhao, F. Tao, H.-L. Li, Journal of Power Sources, 161 (2006) 723-729.
[21] R. de Levie, Electrochimica Acta 9 (9) (1964) 1231-1245.
[22] R. de Levie. Electrochimica Acta 8 (10) (1963) 751-780.
[23] H. Shi, Electrochimica Acta, 41 (1996) 1633-1639.
[24] T.A. Centeno, F. Stoeckli, Journal of Power Sources, 154 (2006) 314-320.
[25] A.T.S. Minori Uchimiya, Geochimica et Cosmochimica Acta, 70 (2006) 1388.
[26] A.S. Viktoria Budavari, Albert Oszko, Mihaly Novak, Electrochimica Acta 48 (2003) 3499.
[27] D.S. May Quan, Mark F. Wasylkiw, and Diane K. Smith, J. Am. Chem. Soc., 129 (2007) 12847.
[28] V. Ruiz, R. Santamaria, M. Granda, C. Blanco, Electrochimica Acta, 54 (2009) 4481-4486.
[29] A.S. A. Rolla, J. Wild, P. Zóltowski, J. Power Sources 5(1980) 189.
[30] Y.N. K. Horita, Y. Nishibori, T. Ohshima, Carbon 34, (1996) 217.

Tables

Figures

Table 1.-Textural and chemical properties of CMs

Sample	Vt	V_{N2}	V_{meso}	L_0	S_{mic}	S_{BET}	TPD		Elemental analysis
							CO_2	CO	O (%)
Super-DLC	0.95	0.63	0.32	1.29	969	1873	0.094	0.368	2.00
A7	0.85	0.75	0.1	0.97	1531	2008	0.230	1.220	4.50
Aerogel	0.58	0.23	0.35	1.15	393	560	0.238	0.002	2.20
MWCNT	2.29	0.08	2.21	2.07	87	210	0.005	0.324	0.50

Vt(cm^3g^{-1}): total volume of pores, V_{N2}(cm^3g^{-1}): total volume of micropores, V_{meso}(cm^3g^{-1}): volume of mesopores, L_0(nm): average pore size S_{mic}(m^2g^{-1}): microporous surface area, S_{BET}(m^2g^{-1}): apparent BET area, TPD (thermal programmed desorption for CO_2 and CO in $mmolg^{-1}$)

Table 2. - Equations that fit the experimental capacitance values and calculated values of C_{dl} and C_p.

Sample	Equation	R^2	C_{dl} (F g^{-1})	C_p/ F g^{-1} (contribution to total capacitance / %)				
				0.2 V	0.4 V	0.6 V	0.8 V	1 V
Super-DLC	$C = 60\Delta V + 108$	0.993	108	12 (10)	24 (18)	36 (25)	48 (31)	60 (36)
A7	$C = 112\Delta V + 150$	0.990	150	22 (13)	45 (23)	67 (31)	90 (38)	112 (43)
Aerogel	$C = 29\Delta V^2 - 2\Delta V + 68$	0.997	68	1 (1)	4 (6)	9 (12)	17 (20)	27 (28)
MWNTs	C = 17	n/a	17	0	0	0	0	0

R^2: correlation coefficient

Figure 1.-
a)

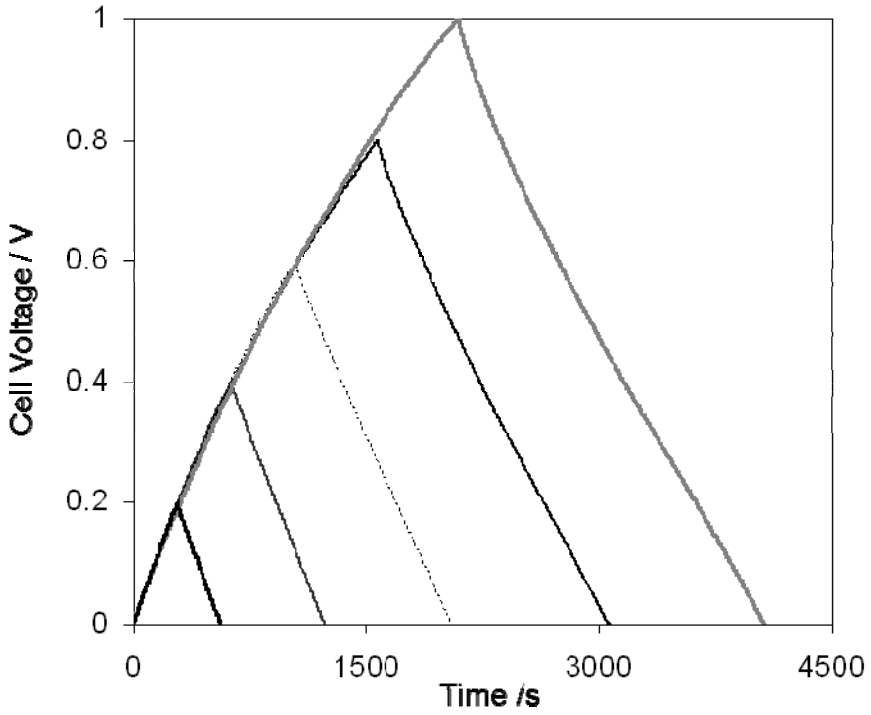
Cell Voltage / V
Time /s
0
0.2
0.4
0.6
0.8
1
0
1500
3000
4500

b)

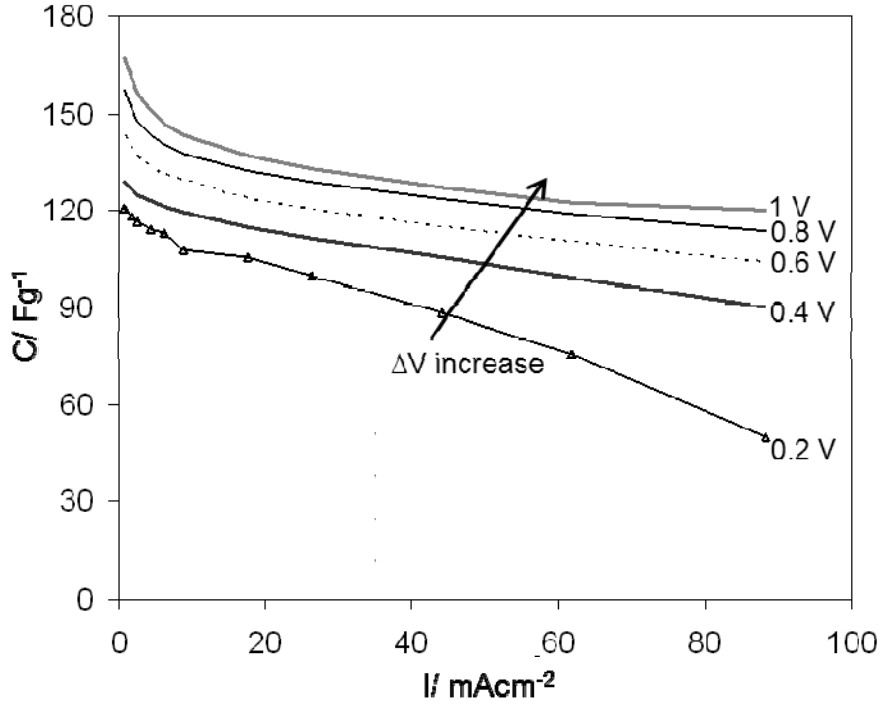
C/ Fg-1
I/ mAcm-2
1 V
0.8 V
0.6 V
0.4 V
0.2 V
ΔV increase
0
30
60
90
120
150
180
0
20
40
60
80
100

Figure 2

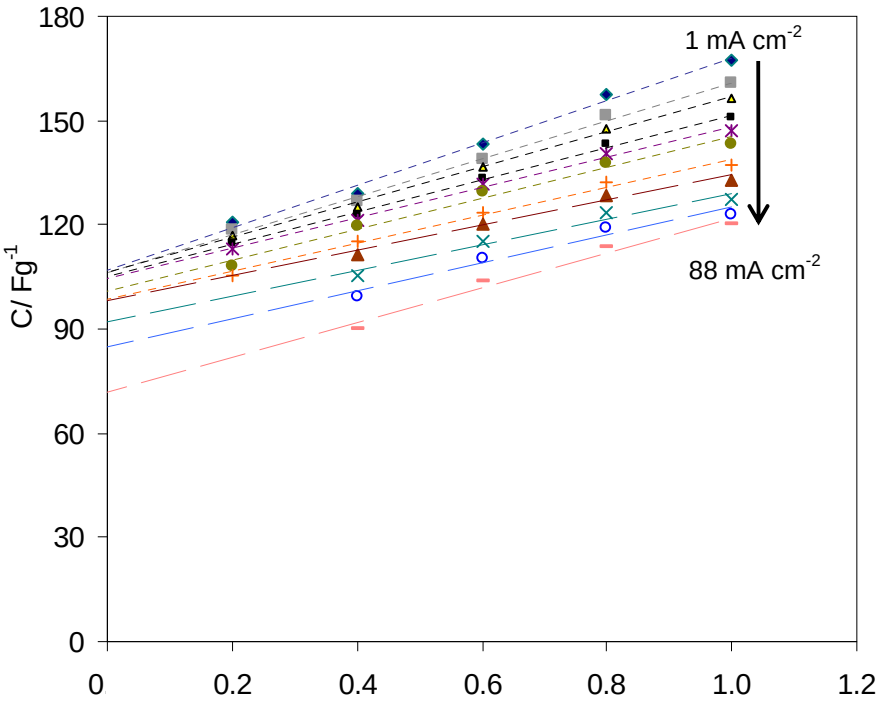

Figure 3

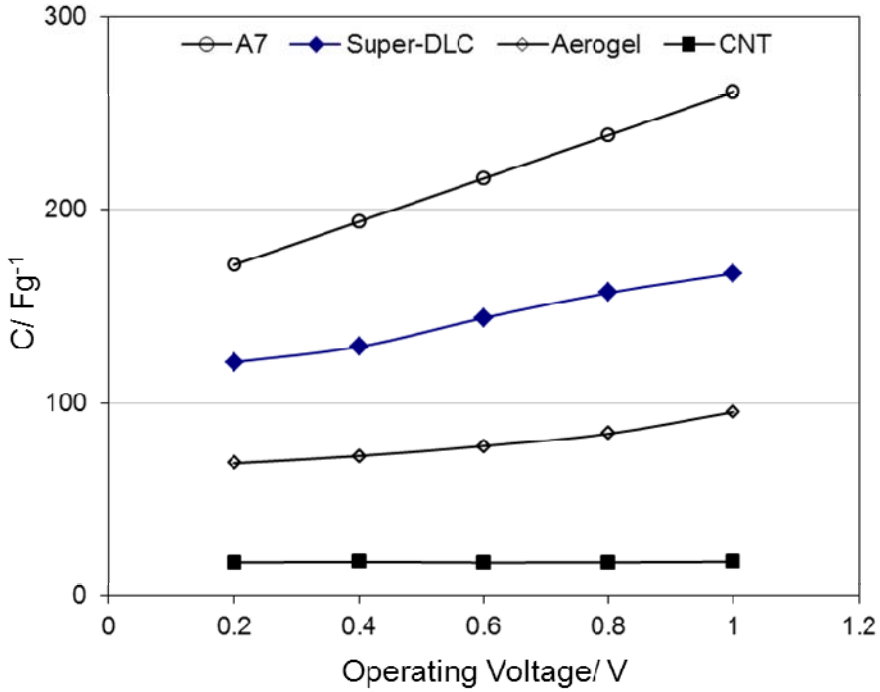
A7
Super-DLC
Aerogel
CNT
300
200
100
0
C/ Fg-1
0
0.2
0.4
0.6
0.8
1
1.2
Operating Voltage/ V

Figure 4.-

a)

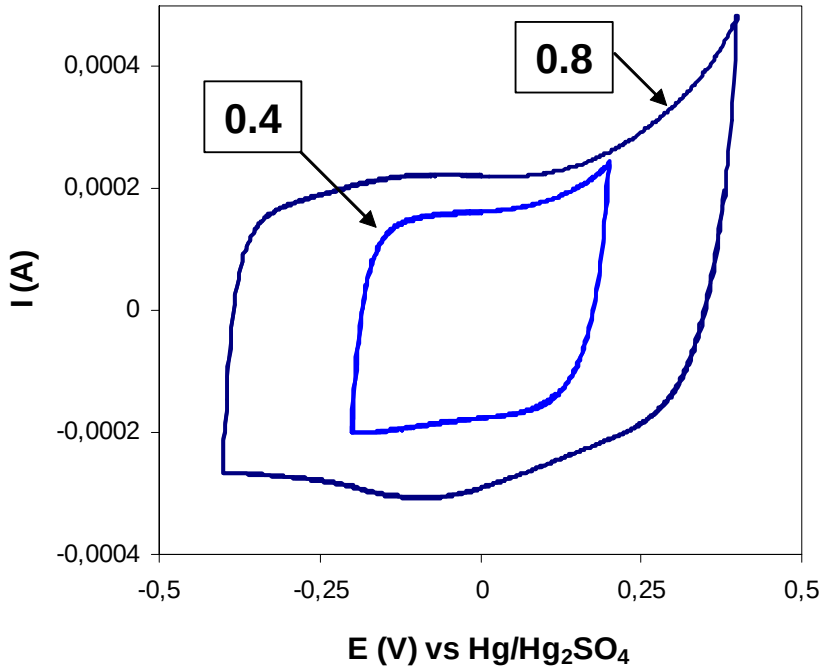
0.8
0.4
0,0004
0,0002
0
-0,0002
-0,0004
I (A)
-0,5
-0,25
0
0,25
0,5
E (V) vs Hg/Hg2SO4

b)

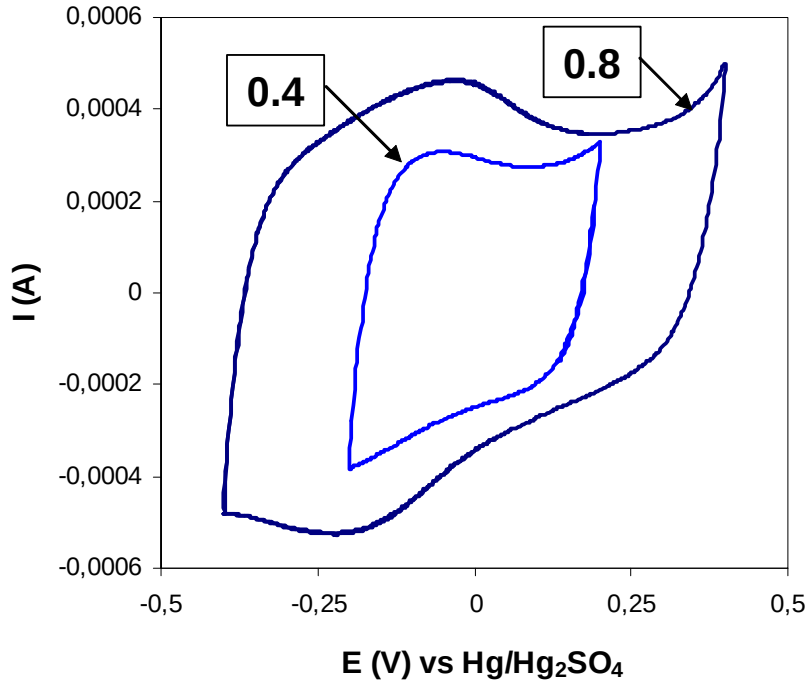
0.8
0.4
0,0006
0,0004
0,0002
0
-0,0002
-0,0004
-0,0006
I (A)
-0,5
-0,25
0
0,25
0,5
E (V) vs Hg/Hg2SO4